Experiments in Fluids manuscript No.
(will be inserted by the editor)

Active and Passive Flow Control on a Precessing Jet

Hamed Babazadeh · David S. Nobes · Charles Robert Koch

Received: 24 September 2014 / Accepted: 24 September 2014 (V7)

Abstract A precessing jet nozzle with water as the working fluid is investigated under passive and active flow control. The actuation effectiveness of twelve microjets around the nozzle inlet for active control of the precessing jet is the focus of this work. Passive control is also applied by modifying the geometry of the precessing jet either by adding a center body near the chamber exit or varying the chamber length. The flow behavior under control is studied using pressure measurement at the chamber exit plane to monitor jet precession. The pressure data is analyzed using a phase plane representation to determine the motion of the jets high velocity region in the chamber exit plane. The standard deviation of the phase of the triggered pressure data is used for stability analysis. This analysis results in a phase diagram in terms of Reynolds number and actuation frequency. Active control can be utilized over a range of actuation frequencies (and corresponding Strouhal numbers) to control precession direction and stability which can be further enhanced with passive control mechanisms. However, the flow follows the actuation with the lowest variation when the active actuation matches with the natural Strouhal number ($0.002<St<0.006$) of the nozzle-jet flow.

Keywords Precessing jet · Active flow control · Phase plane · Real time monitoring

Hamed Babazadeh
E-mail: babazade@ualberta.ca

David S. Nobes
E-mail: david.nobes@ualberta.ca

Charles Robert Koch
Department of Mechanical Engineering
University of Alberta
Edmonton, AB Canada T6G 2G8
E-mail: bob.koch@ualberta.ca

1 Introduction

Jet flows are used to describe any fluid flow in which the flow from a limited space expands and spreads into a free environment with a velocity gradient with respect to the free environment. Fuel injection into a combustion chamber and dispersion of effluent into rivers through a diffuser are examples which can be studied using jet flow models (Green, 1995). A specific configuration of jet flow has found applications as a combustion burner in several industries (e.g. lime, cement) (Nathan et al, 2006). A cylindrical chamber of specific geometry added to the end of a fuel supply pipe introduces an abrupt expansion into the flow. This configuration destabilizes the free jet which leads to a self-excited oscillatory rotational motion, termed *precession* (Nathan et al, 1998), of the entire jet. This rotational motion causes a significant increase in jet entrainment rate and heat transfer from a combusting flame which result in a significant reduction in NO_x emissions (up to 70%), considerable fuel saving (up to 20%) and an improvement in product quality (up to 10%, e.g. in lime industry) (Manias et al, 1996; Nathan et al, 2006).

A precessing jet is a circular axisymmetric jet which initially discharges into a confined pipe, referred to as the chamber (or cavity or shroud) (Nathan et al, 1998) concentric to the jet axis as shown in Fig. 1. The main jet flow reattaches asymmetrically to the wall and then deflects as it leaves the chamber at a large angle to the jet centerline due to the exit lip controlling the spread of the jet. Surface flow visualization techniques in air and water flow visualization have shown that the jet flow reattaches to the chamber wall approximately halfway down the chamber length (Nathan et al, 1998). The deflection angle between the precessing jet and the chamber axis as the jet exits the nozzle is reported to be

$\sim$50° which decreases to 30° at z =0.4D downstream from the chamber outlet plane (Wong et al, 2003). The axis of the jet flow leaving the chamber rotates around the nozzle axis as it exits the chamber and is denoted as the jet in *precessing mode*. Momentary axisymmetric jet flow behavior with reference to the nozzle geometry is denoted as the jet in *axial mode* and can interspersed with the precessing mode (Madej et al, 2011). A passive control mechanism is often applied the form of a *center body* located just upstream from the nozzle exit on the nozzle centerline to restrict the probability of the jet being in axial mode. The presence of this instability and the ability of passive methods to control precession indicates that active control methods may also be appropriate for this flow.

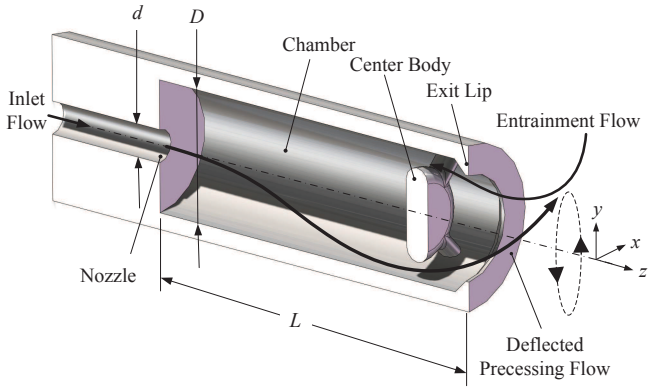

Fig. 1: A sectioned rendered model of a precessing jet nozzle highlighting main geometric parameters.

The main nozzle parameters used to scale a precessing jet are defined in Fig. 1. A precessing jet consists of an axisymmetric jet with a nozzle inlet diameter of d which discharges through a sudden expansion into a confined chamber with a length L and a diameter D such that $D > d$. The Reynolds number of the precessing jet is defined based on the axisymmetric jet entering the cavity as:

$$Re = \frac{\rho U_i d}{\mu} \tag{1}$$

where U_i is the average axial velocity at the nozzle inlet and ρ and μ are the working fluid density and dynamic viscosity, respectively. The frequency of the jet precession is used to define a Strouhal number of the precessing jet as:

$$St = \frac{fd}{U_i} \tag{2}$$

where $f = f_p$ is the frequency of precession. The natural St of the precessing jet reported in the literature to be $St\sim$ 0.003 (Mi and Nathan, 2004) and has been shown to be invariant over a large range of Reynolds number. Numerical simulation has only identified a weak dependence of Strouhal on Reynolds number (Guo et al, 2001). This indicates that the absolute frequency of precession can be assumed a linear function of Reynolds number.

The benefits of using a precessing jet nozzle are inherently linked to the mixing field that it creates beyond the nozzle exit. A mechanical analogue used to investigate the mixing field highlights that in the near field the jet forms an expanding 3D helix which collapses on itself for specific ranges of Strouhal numbers (Nobes, 1998). For $St < 0.008$ based on the nozzle diameter (Mi and Nathan, 2005) the flow never evolves into an axisymmetric jet far downstream of the chamber exit and remains as a rotating, deflected jet. Above this critical value, the precessing jet is only present in the near field of the nozzle exit plane and eventually develops into a simple jet-like regime in the far field. For the naturally occurring phenomenon from a precessing jet nozzle, the mixing field has characteristics of strong three-dimensional motion in the near nozzle region that evolves into a flow with simple-jet like characteristics in the far field (Nathan et al, 2006). Controlling and maintaining this type of mixing field is therefore important to achieve the mixing benefits of a precessing jet nozzle.

Using particle trace flow visualization experiments it was found that a minimum Reynolds number of 3,700 and expansion ratio ($\frac{D}{d} = 3.75$) are needed for precession to occur (Hill et al, 1995). These results highlight that there are a number of conditions related to the nozzle geometry and flow conditions that can influence both whether the flow within the cavity is precessing or not and what frequency of precession is developed by the natural instability.

The flow from the nozzle can also exhibit temporal switching between precessing and axial modes with the probability of being in a certain mode depending on the geometry of the nozzle and flow conditions. Passive stabilization of the precessing mode with introduction of the center body at the chamber exit (see Fig. 1) decreases the probability of the axial mode but does not completely remove it (Wong et al, 2004). A geometric ratio range ($2 \leq \frac{L}{D} \leq 3.5$) for the length of the chamber in which precession occurs is obtained through a parametric study (Nathan, 1988; Newbold, 1998). The effect of chamber length on the probability of a precessing jet shows that the highest probability occurs in a range of $2 \leq \frac{L}{D} \leq 2.75$ but increasing the length ratio causes the probability of jet precession to dramatically reduce (Madej et al, 2011).

Other work has also investigated the use of different inlet conditions into the nozzle chamber on precession stability. The velocity profile at the inlet can be altered by using either an orifice, smooth contraction nozzle and a pipe to deliver jet fluid to the precessing jet chamber (Mi et al, 2006). The results show that the precession frequency is the highest for the orifice flow while lowest for the pipe. The precession Strouhal number of the orifice is double that of the pipe, and is 1.6 times the smooth contraction inlet.

The precession instability observed in the precessing jet is a different phenomenon from jet shear layer instabilities due to the fact that the precession frequency is two orders of magnitude lower than the frequency observed in a shear layer (Nathan et al, 1998). This low frequency precessing frequency is attributed to the jet flow interacting with the chamber to create an absolute instability (Huerre and Monkewitz, 1985). This is unlike convective instabilities in shear layers that grow as they convect downstream. The characteristics of absolute instabilities are more amenable to active control. Control and stabilization of the precession frequency can have significant effects on the jet mixing field. The unstable nature of the precessing jet provides a flow which can potentially be controlled by actuation to excite the flow in a predefined way. Active control of the flow could, therefore, be achieved using a detailed understanding of how to actuate the flow, the limits of actuation and how to monitor the flow for feedback.

This study investigates different active flow control strategies to provide a framework for future feedback control of a precessing jet flow system. The objective of this research is to examine the effectiveness of the actuation on a precessing jet in order to (de)stabilize the jet in precession mode. This can be done because it was established using PIV that 4 pressure sensors at the shroud exit are sufficient to characterize jet precession (Babazadeh et al, 2011). With this simple and perhaps industrially relevant precession measurement system, the conditions for which the active control actuation is effective still needs to be established. To do this a number of major precessing jet nozzle parameters that affect precession and precession stability are systematically varied. A precessing jet configuration either with or without the center body within a chamber length range $2 \leq \frac{L}{D} \leq 3.5$ is investigated under active flow actuation. Twelve micro-jets on the periphery of the inlet into the chamber are used as actuators and pressure data measured at the chamber exit is analyzed using a phase plane representation (Babazadeh et al, 2011) to monitor the direction and characterize the stability of the precession. This provides a comprehensive understanding of the potential to actively actuate the natural instability of a precessing jet nozzle. The active control results are compared to the passive control (using a centerbody) since the passive control provides a baseline to compare the active control. This work is a precursor for developing methods for active control of the mixing field generated by the nozzle.

2 Experimental setup

The general geometry of the nozzle used in this investigation is shown in Fig. 1. To provide actuation 12 micro-jet channels are embedded into the precessing jet nozzle to introduce high velocity fluid into the main jet as it enters the nozzle chamber. The precessing jet shown in Fig. 1 has a center body with a diameter ratio of 0.71 (with respect to the diameter of the chamber). In order to study the effect of the center body (as a passive flow control device), another identical precessing jet was also fabricated without the center body. To facilitate the deflection of the flow while leaving the chamber, a lip with a slope of 45° is mounted in the exit of the chamber (see Fig. 1). This lip also embodies four pressure probes which are used to monitor the location of the precessing jet. The actuation fluid is introduced in the shear layer region of the main jet at the chamber inlet through twelve separate nozzles evenly spaced at circumferential locations through d_{cj}= 0.508 mm (0.02 in) ports. All complex parts are manufactured using a 3D printer (Objet Eden350V, Stratasys Ltd., with a maximum print resolution of 16 μm using FullCure720 material).

Three separate systems are used to generate the main precessing jet flow, provide controlled actuation fluid and to monitor the precessing jet exiting the chamber and these are described in (Babazadeh et al, 2011) with details in (Babazadeh, 2010). The flow facility providing bulk fluid flow (water) to the 5.08 mm nozzle using a progressive cavity pulseless pump which pumps the working fluid in the flow system. The smooth contraction of the plenum and a 20 cm pre-conditioner pipe serves to ensure the inlet flow of the main nozzle chamber is uniform. The flow then exits the nozzle into the chamber and then discharges over the exit chamber lip into the tank which has a pump inlet to return the working fluid back to the pump.

Twelve injectors are used to inject the actuation fluid (room temperature water) which is supplied by a pressure vessel. Using three of the 12 micro-jets simultaneously is found to be effective in controlling the precessing jet and so this pattern is used in this study and is shown in Fig. 2. Three successive injectors (n=3, where n is the number of simultaneously injectors which are on) are always firing and this pattern rotates with a

given frequency (f). In this way the successive pattern (of firing injectors) for CW actuation is:

...,1-2-3, 2-3-4, 4-5-6 ...

and for CCW actuation:

...,1-2-3, 12-1-2, 11-12-1 ...

while the rest of the injectors are turned off. Each of the twelve fuel injectors are calibrated for volume flow rate with this pattern. The result of the calibration gives an average flow rate of 446 ± 25 ml/min.

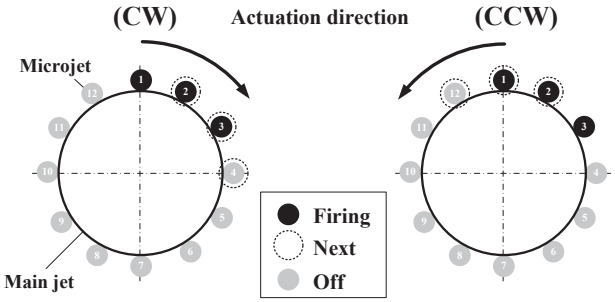

Fig. 2: The firing pattern of the injectors in CW and CCW actuation when three injectors fire simultaneously.

To investigate and monitor the precession phenomenon of the jet exiting the chamber, four probes located near the exit plane of the chamber within the exit lip measure fluid pressure. These probes were located with 90° difference with respect to each other with probe 1 located at the top position and increasing in identification number in the CW direction. Each of the probes is sampled at a rate of 1 kHz. Active flow control is achieved with the injectors while passive control is performed using the center body. In both cases the four pressure probes are used to monitor the location of the precessing jet at the chamber exit – for more details see (Babazadeh, 2010).

The dimensionless parameter which is used to study the behavior of the precessing jet is the Strouhal number (see Eqn. 2), which is the dimensionless frequency. For the Strouhal number, f is either the precessing jet f_p frequency or f the frequency of actuation (i.e. rotation of actuation pattern).

All the test conditions in this work are plotted with actuation frequency f versus Reynolds number and corresponding Strouhal number in Fig. 3. As shown in this figure, all experiments are designed to be conducted around the natural St of the precessing jet which is reported in the literature to be $St\sim$ 0.003 (Mi and Nathan, 2004). The range of values for passive and

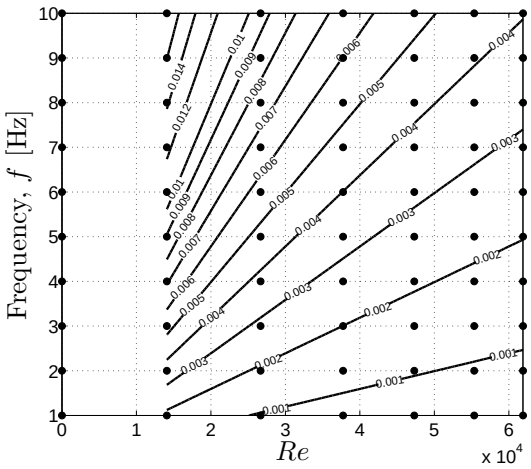

Fig. 3: Measured test points in Reynolds number and frequency plane; the test points in this plane are conducted twenty times (=5 × 2 × 2), for all $\frac{L}{D}$ (5), with and without center body (2) and actuation directions (CW and CW) (2), respectively.

active control is given in Table 1. This results in a 7(Re) × 5(chamber length) × 2(CW/CCW) × 10(f) × 2(CB/no CB) matrix of test conditions (=1400 test points) using the pressure monitoring at the nozzle exit to characterize the precession features of the exiting jet flow. The experimental procedure conducted to collect all data at 1400 test points introduced in Table 1 is detailed in (Babazadeh, 2010). The raw data collected with the pressure sensors is a time series of voltages generated at the four pressure taps located on the periphery of the chamber lip with 90° separation. The data is collected in three stages: when the pump and micro-jets are off, the sensors are only subject to hydrostatic pressure; then with the pump running with micro-jets off, and finally with microjet forcing.

Table 1: The evaluated test conditions

independent variable	**value**
Reynolds number (×1000)	0, 14, 27, 38, 47, 55 and 62
Passive control	with CB and without CB
$\frac{L}{D}$	2, 2.5, 2.75, 3, 3.5
Actuation frequency	1 to 10 Hz (increment:1 Hz)
Actuation direction	CW and CCW

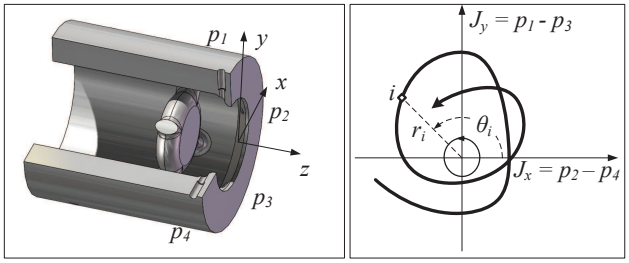

Fig. 4: Location of four pressure probes on the periphery of the chamber and the schematic phase-plane representation of the relative location of jet high velocity region with respect to the probe locations over time; the direction of the curve at the phase plane shows increasing time.

3 Results

A phase plane representation is introduced to investigate the behavior of a precessing jet using only four pressure probes (Babazadeh et al, 2011). Fig. 4 shows the configuration of pressure probes, denoted p_1 to p_4, with respect to each other and the chamber. These probes generate four pressure time series which are mapped into a phase plane formed by the difference between vertical pressure signals on the y-axis ($J_y = p_1 - p_3$) and horizontal signals on the x-axis ($J_x = p_2 - p_4$) as shown in Fig. 4.

An example data set analyzed in this manner is shown in Fig. 5. The complete set of the data represented in this manner for all conditions can be found in Appendix E of (Babazadeh, 2010). The sub-figures showing the locus of pressure are arranged with 10 different actuation frequencies (1-10Hz) in columns; the first three rows with the center-body (w CB) present in the chamber and the second three rows without the center-body (wo CB). For each of these conditions actuation in counterclockwise direction (CCW), clockwise direction (CW) and for no actuation (no act) are shown. The data in Fig.5 is for a constant Reynolds number of 47,000 for two different cavity lengths of $\frac{L}{D} = 2.5$ in Fig. 5(a), to $\frac{L}{D} = 3.5$ in Fig. 5(b). Evidence that the jet is in precession mode is visually apparent in a sub figure when a pressure trace has a regular circular path.

A clear example of the jet in precessing mode is shown in Fig. 5(a) for the conditions a cavity length of $\frac{L}{D} = 2.5$, wCB, CCW for an actuation frequency of 5Hz, despite a pressure trace bias to the top-right, a regular circular pattern with minimal switching across the circular path is observed. Either increasing or decreasing the actuation frequency for this case results in the pressure trace beginning to deviate from this regular circular pattern. At low actuation frequency no clear circular path is present but for higher actuation frequencies a regular path is evident but is not circular in nature.

Increasing the cavity length for the same conditions (the top rows of Fig. 5(b) and comparing to Fig. 5(a)) results in a narrower frequency range of 7-9 Hz over which a circular precessing path is evident. At low actuation frequencies the jet is clearly not strongly precessing. Removing the center body highlights the further the effect of increasing the cavity length from $\frac{L}{D} = 2.5$ to $\frac{L}{D} = 3.5$. In Fig. 5(a), for a shorter cavity length a regular path in the pressure trace is still evident, (in rows 5 and 6) albeit not circular in shape. For the longer cavity length (In Fig. 5(b) rows 5 and 6), there is no regular shape in the pressure trace indicating that precession or motion of the jet in a regular manner is not strongly evident. This influence of cavity length is also apparent for the no actuation case with the pressure trace showing a patterned shape strongly with the presence of a center body (w CB, no act – Fig. 5(a) and (b) row 3) but also evident for no center body (wo CB, no act – Fig. 5(a) and (b) row 6). While this figure provides visual feedback of the stability of precession under different conditions a more quantitative approach is needed and that is given next.

A measure of the average value of the radial position in the phase plane $\bar{r}$ is calculated for all Reynolds numbers and chamber length ratios ($\frac{L}{D}$) with and without actuation as:

$$\bar{r} = \frac{1}{n} \sum_{i=0}^{n} r_i \tag{3}$$

To see the phase plane behavior and to remove the dynamic pressure effect on $\bar{r}$ value due to Reynolds number, $\bar{r}$ is normalized by the dynamic pressure corresponding to the inlet velocity of the main jet at the nozzle inlet. R_n is defined as:

$$R_n = \frac{\bar{r}}{\frac{1}{2}\rho U_i^2} \tag{4}$$

Values of R_n as a function of chamber length for six Reynolds numbers and with and without center body are plotted in Fig. 6. As expected, without the center body, all curves are grouped together and R_n decreases as $\frac{L}{D}$ increases. With the center body, the different Reynolds number lines are not as closely grouped. For $\frac{L}{D} = 2$, R_n is smaller than for $\frac{L}{D} = 2.5$ and here it is speculated that this might be due to the presence of a strong axial mode cavity oscillation at this cavity length.

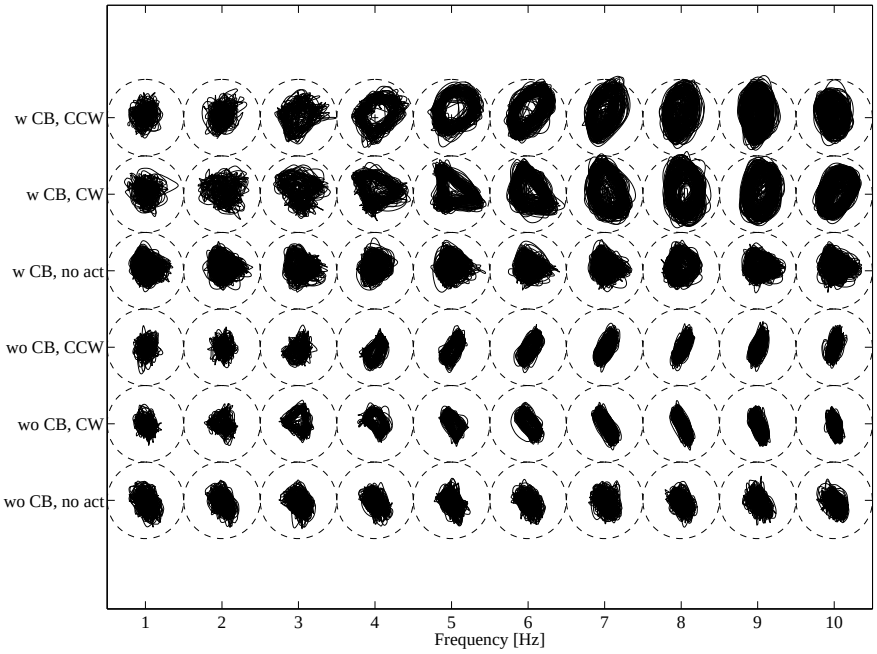

(a)

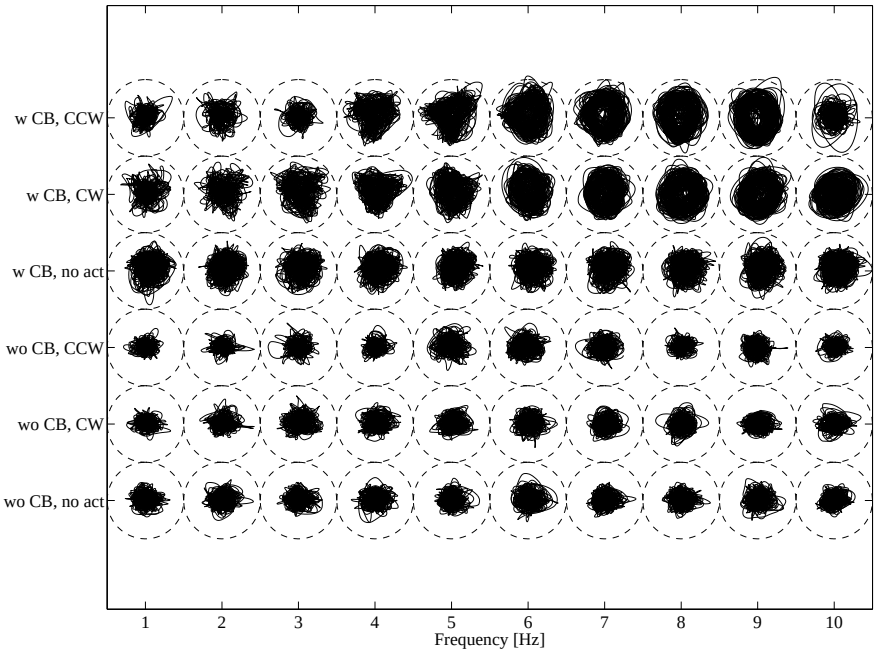

(b)

Fig. 5: Pressure Phase plane data obtained at $Re = 47,000$ with f varying from 1 to 10 Hz for: with center body (w CB) and without center body (wo CB) each with: CCW, CW and no actuation (no act) (a) $\frac{L}{D} = 2.5$, (b) $\frac{L}{D} = 3.5$. (Babazadeh, 2010) App. E

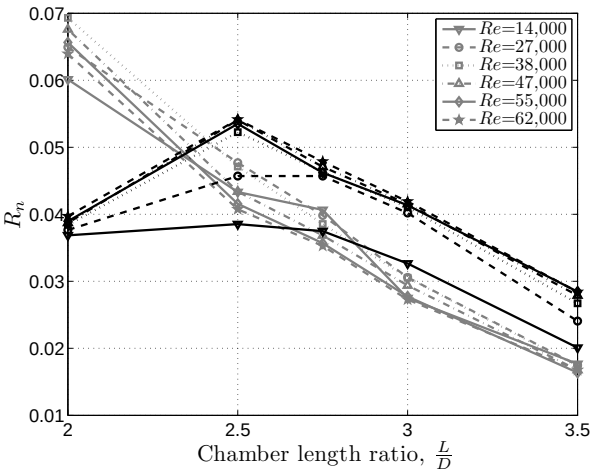

Fig. 6: The influence of chamber length on the dynamic pressure normalized value (gray: without center body, black: with center body).

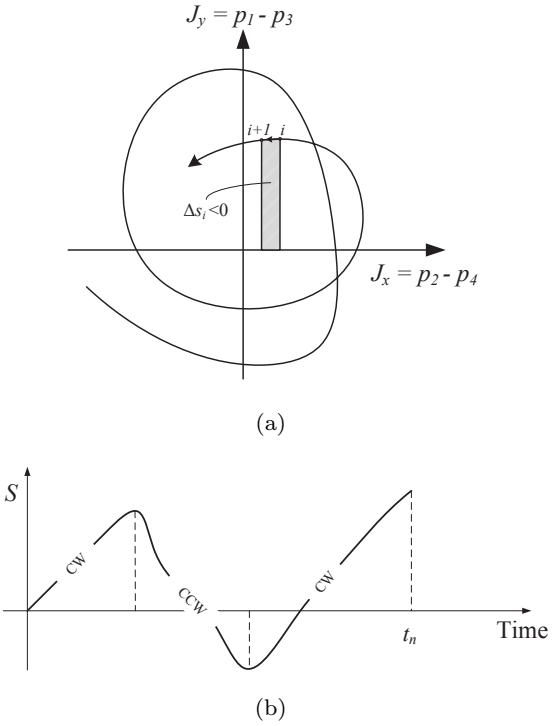

Fig. 7: (a) Integration method to calculate the direction of precession based on phase plane mapping. (b) Schematic representation of S value versus time; the slope of S indicates the direction of the precession such that the positive and negative S values show CW and CCW precession, respectively.

To extract the direction of precession from the phase plane, the integration of phase plane curve is calculated for each time step as shown in Fig. 7(a) using:

$$\Delta s_i = \frac{1}{2}[(J_{x,i+1} - J_{x,i})(J_{y,i} + J_{y,i+1})] \tag{5}$$

then the integration of this curve from initial time is calculated:

$$S(t_n) = \sum_{i=0}^{n} \Delta s_i \tag{6}$$

An example of the variation of $S(t_n)$ as a function of time is plotted in Fig. 7(b). The positive and negative slopes of S correspond to CW and CCW precession, respectively. This method is used in this study to investigate the direction of precession over time.

The direction analysis, using Eqns. 5 and 6, for several Reynolds numbers are shown in Fig. 8. Increasing Reynolds number increases the dynamic pressure and thus the pressure difference for a precessing jet. This, in turn, causes larger x and y values in the phase plane and so Δs_i in Eqn. 5 is larger, resulting in a larger slope in Eqn. 6. More importantly, Fig. 8 indicates that the jet precession in this setup has a preferred direction before actuation (first 40 s) which is CW: the flow is actuated CCW direction by the prior knowledge of this preferred CW direction. At $t = 40$ s, CCW actuation is applied and the direction of precession switches to CCW for low Re. However, at high Reynolds numbers, precession resists switching directions ($Re \geq 55,000$) and at $Re = 62,000$, the actuation does not affect the precession direction. At these Reynolds numbers, the applied actuation is not able to reverse the preferred precession direction.

One main objective of the pressure data analysis is to determine a measure to evaluate the actuation effectiveness on the precession phenomenon. This measure should be able to evaluate the actuation effectiveness at each test point and to compare the actuation effectiveness over the entire range of test points. During the experiments, the command signal of the injector 1 was collected. It was used as a trigger for the pressure signals providing data which are synchronous with the actuation pattern. A typical data set has between 20 to 200 trigger points for the actuation frequency $f = 1$ Hz to $f = 10$ Hz, respectively. These triggered data points can then displayed on a phase plane as in Fig. 9 for two different test points. High actuation effectiveness is defined as when the flow follows the actuation faithfully as shown in Fig. 9(a) where the trigger points are clustered close to the centroid location of these points. A test point where the actuation is not able to manipulate the precessing jet effectively is shown in Fig. 9(b).

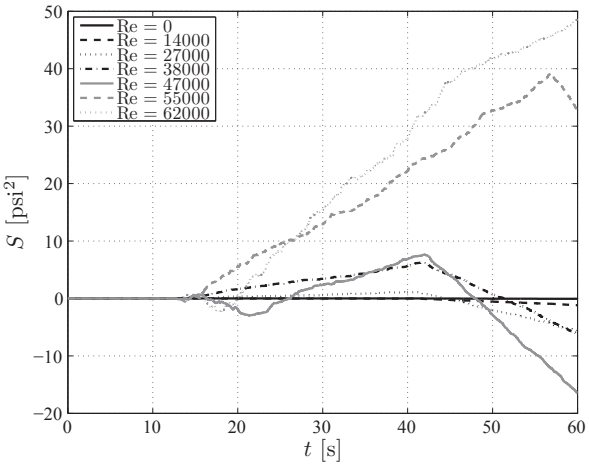

Fig. 8: Direction analysis for the CCW actuation of the flow with the chamber length ($\frac{L}{D}$) of 2.5 at $f = 6Hz$; CW is the preferred direction of precession; also it shows the effect of Reynolds number on actuation effectiveness, i.e. the ability to change the precession direction.

There is a large spread of the trigger points over the phase plane indicating a wide variation in jet location and precession frequency.

To quantify these observations, the standard deviation of the phase angle (θ_{STD}) of these points from their centroid (shown in Fig. 9 by ♦) is determined to give a measure of scattering of these points in the azimuthal direction. Fig. 10 and Fig. 11 show the standard derivation of the location of the precessing jet for a short ($\frac{L}{D} = 2.5$) and long chamber ($\frac{L}{D} = 3.5$), respectively. Both of these figures show without a center body in sub-figures (a) and (b) and with a center body in sub-figures (c) and (d). The colorbar represents the relative value of θ_{STD} and darker values indicate that θ_{STD} increases. Therefore, bright regions represent regions in the parameter space where the actuation is effecting the flow and is stabilizing precession. Fig. 10 and Fig. 11 show that the flow manipulation by high actuation frequency at low Reynolds numbers and low frequency in high Reynolds numbers result in a large value of θ_{STD} indicating the flow can not be properly controlled in these regions.

Since a similar θ_{STD} pattern in the $Re - f$ plane in Fig. 10 and Fig. 11 is observed, an average of all ten diagrams (5(chamber lengths) × 2(CW,CCW)) is generated and results in a general phase-diagram for actuation effectiveness on a precessing jet which is shown in Fig. 12. All test points and the results for a chamber without center body are given in Fig. 12(a) and with

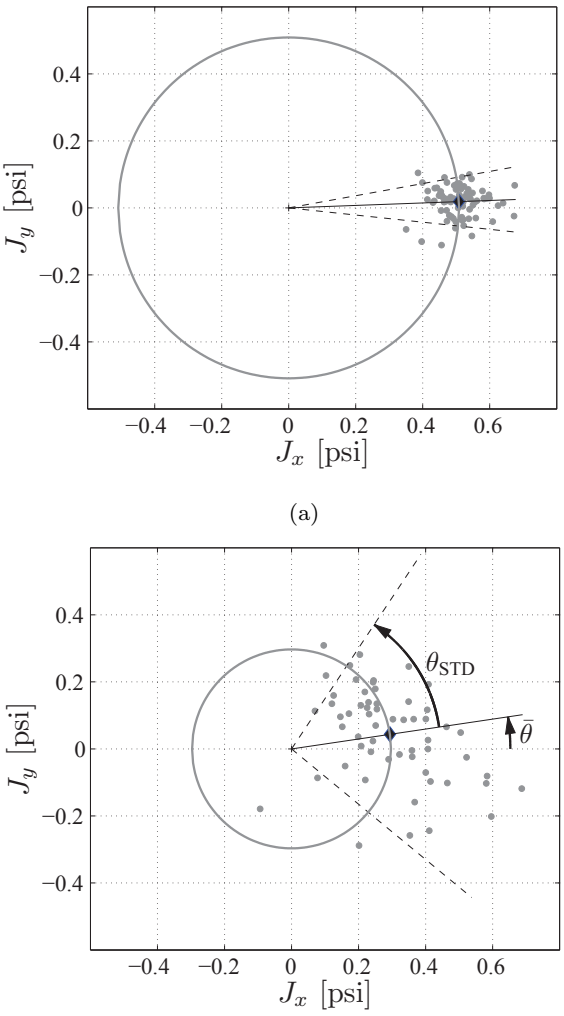

Fig. 9: Phase plane representation of the triggered pressure data and the standard deviation of their phase with respect to their centroid point (shown in figures by at $\frac{L}{D}$=2, without center body, CW actuation for (a) Re=27,000, f=4 Hz and (b) Re=38,000, f=3 Hz.

center body in Fig. 12(b). Both diagrams have a similar pattern such that the deviation (θ_{STD}) increases at the right bottom and left top corner in the $Re - f$ plane. In other words, low frequency actuation does not manipulate the main jet flow at a high Reynolds number and vise vera. The Strouhal number corresponding to the actuation frequency (Eqn. 2) is also plotted in Fig. 12. The light zones indicate the effective of actuation on controlling the precessing jet while dark zones indicate poor actuation effectiveness. As expected, the Strouhal number range in which the flow can be effectively actu-

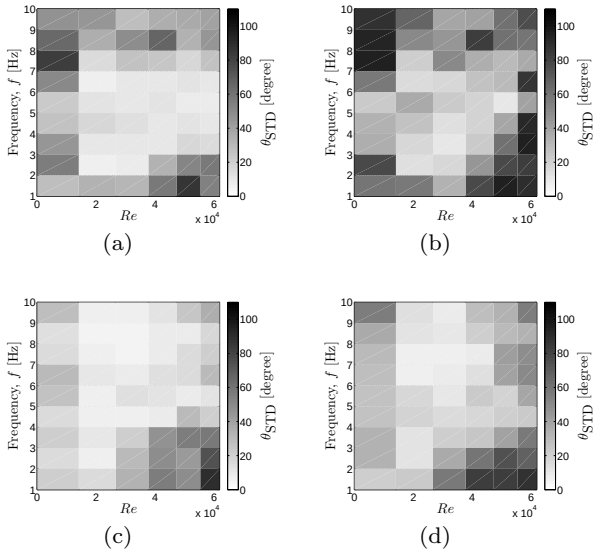

Fig. 10: The influence of Reynolds number and frequency on STD of phase of the triggered pressure data at the chamber length ratio $\frac{L}{D}$=2.5. Without center body: (a) CW, (b) CCW actuation. With center body: (c) CW and (d) CCW actuation.

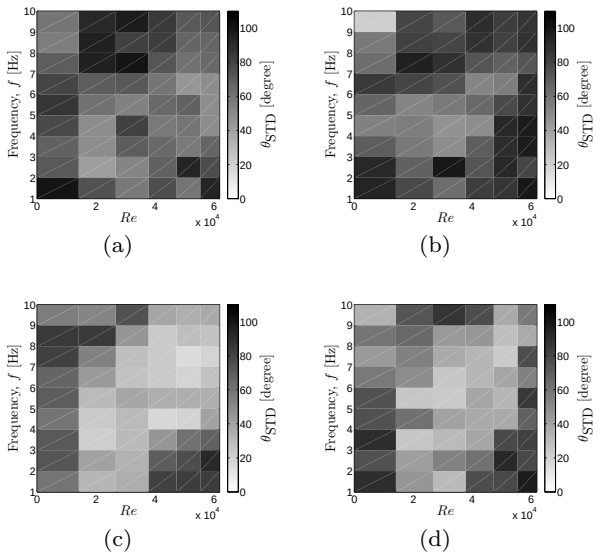

Fig. 11: The influence of Reynolds number and frequency on STD of phase of the triggered pressure data at the chamber length ratio $\frac{L}{D}$=3.5. Without center body: (a) CW, (b) CCW actuation. With center body: (c) CW and (d) CCW actuation.

ated overlaps with $0.002 \leq St \leq 0.006$ associated with the natural frequency of precession.

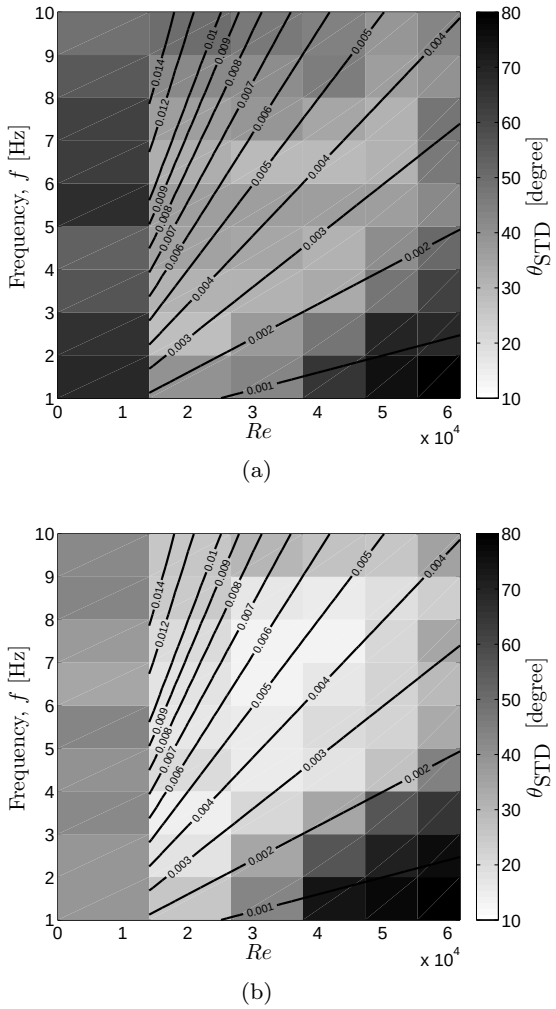

Fig. 12: The influence of frequency and Reynolds number of on STD of phase of the triggered pressure data averaged for $2.0 \leq \frac{L}{D} \leq 3.5$ for (a) without center body and (b) with center body; the contour lines show St on Re-f plane.

Focusing on the chamber length, θ_{STD} increases with increasing chamber length indicating that actuation effectiveness for the long chambers is lower than for short chambers as shown in Fig. 13. Fig. 13 also reveals that adding a center body stabilizes the precession phenomenon. This effect can also be observed by comparing the overall intensity in Fig. 12(a) and Fig. 12(b). In addition, Fig. 13 confirms that the actuation in the preferred direction (CW) is more effective than the CCW direction. The curves with $\bigtriangledown$ (with the center body and CW actuation) and $\circ$ (without the center body and CCW actuation) in Fig. 13 illustrate the competition between the influence of the center body and the actuation direction on the precession stabil-

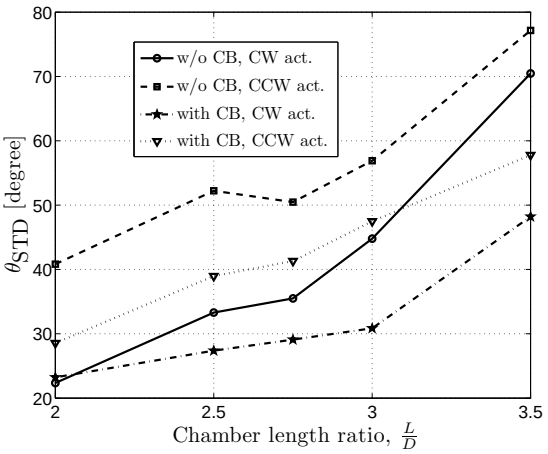

Fig. 13: The influence of chamber length ratio ($\frac{L}{D}$) on STD of phase of the triggered pressure data averaged for all frequencies and Reynolds number.

ity. It can be concluded from Fig. 13 that for chamber lengths $\frac{L}{D} \leq 3$, the effect of actuation direction dominates the effect of the center body while for $\frac{L}{D} = 3.5$, the chamber with the center body in the CCW direction presents a more stable precession.

Looking more carefully at Figs. 12(a) and 12(b), there is slight differences in θ_{STD} (color intensity) between with center body and no center body cases. Having a center body decreases the deviation (θ_{STD}) indicating better control effectiveness with the center body. This effect can also be observed by comparing the overall intensity in Fig. 12(a) and Fig. 12(b). In Fig. 13, the deviation of CW is less that CCW actuation confirming the already observed CW preferred direction.

These results also show that open loop active control of the precessing jet using 12 micro-jets has been found to be effective when the actuation matches the instability mode of the chamber. Furthermore, 4 pressure taps mounted to the shroud exit are able to observe the precessing of the jet at the shroud exit and thus provide a measurement that could be used in a feedback control. This control has not yet been implemented but could consist of either: (1) feedback control to perhaps lock to a swirling frequency despite upstream jet flow changes; or (2) a type of control that optimizes mixing perhaps using extremum seeking methods (Schneider et al, 2000).

Conclusions

The instability of a precessing jet for several different nozzle configurations has been investigated under the influence of controlled actuation. An *in situ* monitoring system based on phase plane pressure measurements has been used to identify the real-time state of the jet exiting the nozzle (Babazadeh et al, 2011). Phase plane representation reveals the direction and stability of the precessing jet under actuation. The direction of precession is found by integration on this plane and the standard deviation of the phase of triggered pressure data is used to quantify precessing stability. A phase diagram is constructed based on the stability analysis which shows that actuation at the Strouhal number corresponding to the natural Strouhal number of the precessing jet is most effective. This natural frequency of the nozzle is a function of both the nozzle configuration and flow rate of the working fluid. The actuation strategy is able to control the direction and stability of precession over a range of lower Reynolds numbers but at high Reynolds numbers where the flow has significant momentum, the jet continues to precess in its preferred direction despite control jet inputs. The experimental establishment of the effectiveness of the 12 jet micro-actuation on jet precession over a range of flow Reynolds numbers, forcing frequencies and chamber lengths is one main result of this work. In future work, we hope to combine the developed 4 probe measurement system with the knowledge of the actuation effectiveness in novel feedback control of a precessing jet to either stabilize or destabilize the jet precession.

Acknowledgments The authors acknowledge funding support for this research from the Alberta Ingenuity Fund, the Natural Sciences and Research Council (NSERC) of Canada and the Canadian Foundation for Innovation (CFI).

References

Babazadeh H (2010) Active flow control of a precessing jet. M.Sc. thesis, University of Alberta

Babazadeh H, Koch CR, Nobes DS (2011) Investigation of micro-jet active control of a precessing jet using PIV. Experiments in Fluids 51(6):1709–1719

Green S (ed) (1995) Fluid Vortices. Academic Publishers

Guo B, Langrish T, Fletcher D (2001) Numerical simulation of unsteady turbulent flow in axisymmetric sudden expansions. J Fluids Eng 123:574–587

Hill S, Nathan G, Luxton R (1995) Precession in axisymmetric confined jets. In: 12th Australasian Fluid Mechanics Conference

Huerre P, Monkewitz P (1985) Absolute and convective instabilities in free shear layers. Journal of Fluid Mechanics 159:151–168

Madej A, Babazadeh H, Nobes DS (2011) The effect of chamber length and reynolds number on jet precession. Experiments in Fluid 51(6):1623–1643

Manias C, Balendra A, Retallack D (1996) New combustion technology for lime production. World Cement 27(12):34–39

Mi J, Nathan G (2004) Self-excited jet-precession strouhal number and its influence on downstream mixing field. Journal of Fluids and Structures 19:851–862

Mi J, Nathan G (2005) Statistical analysis of the velocity field in a mechanical precessing jet flow. Phys Fluids 17:015,102–17

Mi J, Nathan G, Wong C (2006) The influence of inlet flow condition on the frequency of self-excited jet precession. Journal of Fluids and Structures 22:129–133

Nathan G (1988) The enhanced mixing burner. PhD thesis, University of Adelaide

Nathan G, Hill S, Luxton R (1998) An axisymmetric nozzle to generate jet precession. Journal of Fluid Mechanics 370:347–380

Nathan G, Mi J, Alwahabi Z, Newbold G, Nobes D (2006) Impacts of a jet's exit flow pattern on mixing and combustion performance. Progress in Energy and Combustion Science 32(5-6):496–538

Newbold G (1998) Mixing and combustion in precessing jet flows. PhD thesis, University of Adelaide

Nobes DS (1998) The generation of large-scale structures by jet precession. PhD thesis, University of Adelaide

Schneider G, Ariyur K, Krstic M (2000) Tuning of a combustion controller by extremum seeking: a simulation study. Decision and Control, 2000 Proceedings of the 39th IEEE Conference 5:5219–5223 vol.5

Wong C, Lanspeary P, Nathan G, Kelso R, O'Doherty T (2003) Phase-averaged velocity in a fluidic precessing jet nozzle and in its near external field. Experimental Thermal and Fluid Science 27:515–524

Wong C, Nathan G, O'Doherty T (2004) The effect of initial conditions on the exit flow from a fluidic precessing jet nozzle. Experiments in Fluids 36:70 – 81